

# Poly(diethylsiloxane-*co*-diphenylsiloxane) and poly(diethylsiloxane-*co*-3,3,3-trifluoropropylmethylsiloxane): synthesis, characterization and low-temperature properties

J. R. Brewer\*, K. Tsuchihara and R. Morita

*National Institute of Materials and Chemical Research, 1-1 Higashi, Tsukuba 305, Japan*

and J. R. Jones and J. P. Bloxside

*Department of Chemistry, University of Surrey, Guildford, Surrey, GU2 5XH, UK*

and S. Kagao and T. Otsuki

*Toyo Ink MFG Co. Ltd, Tsukuba Research Laboratories, 27 Wadai, Tsukuba 305, Japan*

and S. Fujishige

*Tokyo Kasei University, 1-1-18 Atabashi, Kaga, Tokyo 173, Japan*

*(Received 5 April 1994)*

Copolymers containing diethylsiloxane and functional siloxane groups of the form  $RR'SiO$  (where R, R' = phenyl, and R = methyl, R' = 3,3,3-trifluoropropyl) were synthesized by equilibrium polymerization of the appropriate cyclotrisiloxanes in the presence of KOH. Quantitative  $^{29}Si$  n.m.r. spectroscopy indicated that the copolymers possessed random microstructures. D.s.c. and dynamic mechanical analysis show that both substituents are effective in lowering the crystal melting and low-temperature crystal-crystal transitions with respect to the diethylsiloxane homopolymer, and ultimately lead to non-crystalline copolymers.

(Keywords: siloxane copolymers;  $^{29}Si$  n.m.r. spectroscopy; poly(diethylsiloxane))

## INTRODUCTION

In recent years the application of elastomers, particularly polysiloxanes, to sealant applications in severe environments has become widespread<sup>1</sup>. In cryogenic applications, such as 'O' rings for liquid oxygen tanks, a variety of alkyl and halogenated siloxanes have been evaluated<sup>2</sup>. However, the low-temperature performance of the materials that are available is still considered to be, at best, only adequate. Copolymers of dimethylsiloxane and 3,3,3-trifluoropropylmethylsiloxane are currently regarded as the best materials for low-temperature use<sup>3</sup>. The dimethylsiloxane component provides excellent main chain flexibility and a low  $T_g$  ( $-123^\circ C$ ), whereas the fluorinated group eliminates the tendency of the dimethyl segment to crystallize at  $-54^\circ C$ . Consequently, crystallization-free copolymers, with glass transition temperatures as low as  $-115^\circ C$ , have been obtained<sup>4,5</sup>. Similarly, the incorporation of low levels of phenyl groups (up to 8%) has been shown to lower the stiffening temperatures in Gehmann cold twist experiments<sup>6</sup>. At higher phenyl

contents, a steady increase in the stiffening temperatures was observed.

Polydiethylsiloxane (PDES) is the most extensively studied member of a series of liquid crystalline polymers, including polydipropylsiloxane<sup>7-9</sup> and polyphosphazenes<sup>10-12</sup>, which contain inorganic chain backbones and organic side-chain groups. Due to the flexibility of the Si-O bond and facile rotation of the side chains around the Si-C bond, high-molecular-weight PDES has the extremely low glass transition temperature of  $-138^\circ C$ , which is the lowest known for high-molecular-weight polymers. Although the low-temperature, first-order transition behaviour of PDES has been extensively studied by d.s.c.<sup>13-20</sup>, X-ray diffraction<sup>15,17,20,21</sup>, Raman spectroscopy<sup>22</sup>, adiabatic calorimetry<sup>21</sup> solid-state n.m.r. spectroscopy<sup>17,18,23,24</sup>, dielectric measurements<sup>17,25</sup> and molecular simulation<sup>26</sup>, there are no publications dealing with the modification of the crystal structure by copolymerization. In this present paper we report the synthesis, characterization and low-temperature properties of poly(diethylsiloxane-*co*-diphenylsiloxane) and poly(diethylsiloxane-*co*-3,3,3-trifluoropropylmethylsiloxane), denoted by poly(DES-*co*-DPS) and poly(DES-*co*-TFPMS), respectively.

\*To whom correspondence should be addressed

## EXPERIMENTAL

## Synthesis of copolymers

All copolymers were prepared by the equilibrium polymerization of mixtures of the appropriate cyclo-trisiloxanes, catalysed by KOH. Since there is a large difference in reactivity between the diethyl ( $E_3$ ), and the diphenyl ( $P_3$ ) and trifluoropropylmethyl ( $F_3$ ) trimers, reactions were conducted at elevated temperature (160°C) for 24 h to allow full equilibration to be achieved. It was found that  $E_3$  and  $P_3$  were incompatible, so equilibrations were therefore carried out in the presence of a cosolvent, octaethylcyclotetrasiloxane ( $E_4$ ), which did not polymerize under the conditions employed. In order to control the molecular weight and sharpen the molecular weight distribution, the copolymerizations were conducted in the presence of the difunctional chain stopper, 1,3-divinyl-1,3-diphenyl-1,3-dimethyldisiloxane. Molecular weights were kept low ( $< 20\,000$ ) in order to facilitate quantitative analysis by  $^{29}\text{Si}$  n.m.r. spectroscopy, including the chain ends.

 $^{29}\text{Si}$  n.m.r. spectroscopy

$^{29}\text{Si}$  n.m.r. spectra were obtained on a Bruker AC300 spectrometer operating at 59.6 MHz. Typically, a solution of chromium acetylacetonate ( $\text{Cr}(\text{acac})_3$  (0.1 M) was added in order to suppress nuclear Overhauser enhancements (n.O.es) and to shorten the  $T_1$  spin-lattice relaxation times. The latter were checked by the inversion-recovery method and were generally less than 1 s. Therefore, to satisfy the condition for quantitative spectra, i.e. pulse interval  $> 5T_1$ , a standard pulse interval of 5 s was used. In order to ensure equal suppression of the n.O.es, spectra were acquired with gated decoupling (decoupler off throughout the pulse interval) in order to allow the residual n.O.es to decay. All spectra were recorded in benzene- $d_6$  solution and chemical shifts are quoted relative to tetramethylsilane (TMS).

## Molecular weight measurements

Vapour phase osmometry was carried out at 35°C using a Corona 117 instrument, with chloroform as the solvent. Apparent molecular weights were obtained via size exclusion chromatography (s.e.c.) in tetrahydrofuran

(THF) at 40°C with the use of a Tosoh 8020 liquid chromatograph equipped with Styragel columns.

## Calorimetry

D.s.c. measurements were recorded using a Seiko SII instrument which had previously been calibrated using samples of high-purity indium. In all cases, the sample (10 mg) was isotropized at 50°C for 10 min before the cooling run was started, in order to remove any thermal memory effects. (PDES samples are renowned for showing d.s.c. behaviour dependent on their previous thermal history.) Samples were cooled to  $-180^\circ\text{C}$  at rates of either  $8^\circ\text{C}$  or  $2.5^\circ\text{C min}^{-1}$  and such runs are denoted by fast and slow cooling, respectively. In all cases an equilibration period of 10 min was followed by heating at a rate of  $10^\circ\text{C min}^{-1}$ .

## Viscoelasticity

Viscoelastic behaviour was studied using a Rheometrics RDS-II dynamic mechanical spectrometer, using parallel plate geometry in cure mode. Due to the differences in torque imparted by the samples, 12.5 mm diameter fixtures with a strain range of 1–100% were used for amorphous samples, whereas a smaller (4 mm) fixture (strain range of 0.1–1%) was employed in the case of crystalline samples.

## RESULTS AND DISCUSSION

The composition and molecular weights of all of the copolymers studied in this work are given in Table 1. Perusal of the data indicates that the observed comonomer contents are similar to the feed ratios, thus indicating that equilibrium has been reached. Attempts to prepare copolymers with 30% phenyl content were unsuccessful, since the reaction mixture rapidly became heterogeneous after addition of the catalyst. This is attributed to the formation of blocks of high diphenyl-siloxane content which are not compatible with the much less reactive  $E_3$  comonomer or the cosolvent. In the case of the copolymers with  $F_3$ , the reaction mixture remained homogeneous throughout the reaction and copolymers containing high levels of  $F_3$  were readily prepared.

Table 1 Composition and properties of poly(DES-co-DPhS) and poly(DES-co-TFPMS) copolymers<sup>a</sup>

Polymer	$X^b$	Feed <sup>b</sup> (%)	Found <sup>c</sup> (%)	$\bar{M}_n^d$ ( $\times 10^4$ )	$\bar{M}_n^e$ ( $\times 10^4$ )	$\bar{M}_w^e$ ( $\times 10^4$ )	$\bar{M}_w/\bar{M}_n^e$	$T_g$ (°C)	Type
EP1	$P_3$	0.50	0.45	1.52	1.83	2.86	1.56	-136.0	Crystalline
EP2	$P_3$	1.25	1.00	1.54	1.80	3.13	1.74	-134.9	Crystalline
EP3	$P_3$	2.50	2.19	1.85	1.90	2.94	1.55	-133.7	Crystalline
EP4	$P_3$	5.00	4.88	1.48	1.72	2.72	1.58	-131.0	Crystalline
EP5	$P_3$	10.00	8.15	1.73	1.76	3.48	1.98	-127.3	Amorphous
EF1	$F_3$	5.00	4.21	–	1.95	3.18	1.63	-134.7	Crystalline
EF2	$F_3$	10.00	8.40	1.46	1.62	2.73	1.68	-132.6	Crystalline
EF3	$F_3$	15.00	12.20	–	1.30	2.37	1.82	-133.9	Borderline
EF4	$F_3$	25.00	23.40	1.58	1.25	2.20	1.76	-128.0	Amorphous
EF5	$F_3$	50.00	49.62	–	1.23	1.68	1.37	-109.7	Amorphous

<sup>a</sup>Mole ratio of monomers (total)/catalyst = 1580/1; mole ratio of monomers (total)/chain stopper = 110/1

<sup>b</sup> $X$  = functional comonomer

<sup>c</sup>Determined by  $^1\text{H}$  n.m.r.

<sup>d</sup>Determined by vapour phase osmometry

<sup>e</sup>Determined by s.e.c.

The microstructures of the copolymers were examined by  $^{29}\text{Si}$  n.m.r. spectroscopy. The main-chain region of the quantitative  $^{29}\text{Si}$  n.m.r. spectrum of the copolymer EF5 (Figure 1) comprises two multiplet signals, at  $-19.0$  and  $-22.2$  ppm, respectively. Assignment of the downfield signal to the diethylsiloxane unit was made by reference to the chemical shift of the PDES homopolymer. Similar treatment confirmed the assignment of the upfield signal to the trifluoropropylmethylsiloxyl group. If the diethylsiloxane signal is considered first, for a random copolymer, the silicon nucleus is affected in three different ways, according to the triad structures I–III (Table 2).

Statistically, there are two ways of forming the central triad II, therefore its intensity is doubled and the n.m.r. signal assumes the shape of a triplet. This is clearly seen in the spectrum, along with fine splitting which is due to

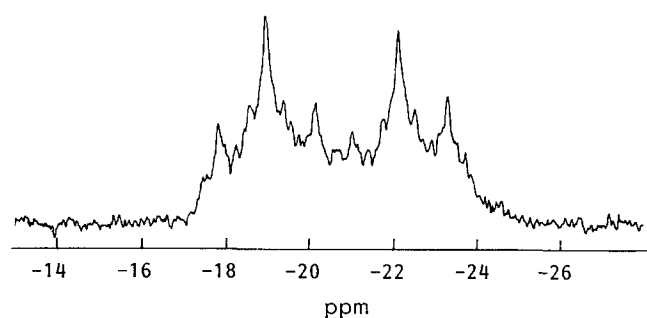


Figure 1 Main-chain region of the  $^{29}\text{Si}$  n.m.r. spectrum of the copolymer EF5

Table 2 Triad sequences for EF copolymers

Triad	Sequence
I <sup>a</sup>	–SiMePr <sub>r</sub> O–SiEt <sub>2</sub> O–SiMePr <sub>r</sub> O–
II <sup>a</sup>	–SiMePr <sub>r</sub> O–SiEt <sub>2</sub> O–SiEt <sub>2</sub> O–
III <sup>a</sup>	–SiEt <sub>2</sub> O–SiEt <sub>2</sub> O–SiEt <sub>2</sub> O–
IV <sup>b</sup>	–SiMePr <sub>r</sub> O–SiMePr <sub>r</sub> O–SiMePr <sub>r</sub> O–
V <sup>b</sup>	–SiMePr <sub>r</sub> O–SiMePr <sub>r</sub> O–SiEt <sub>2</sub> O–
VI <sup>b</sup>	–SiEt <sub>2</sub> O–SiMePr <sub>r</sub> O–SiEt <sub>2</sub> O–

<sup>a</sup>E-centred triads

<sup>b</sup>F-centred triads

Table 3 Experimental and calculated run numbers of poly(DES-co-DPhS) and poly(DES-co-TFPMS)

Polymer	X <sup>a</sup>	E content (%)	X content (%)	R <sub>E</sub> <sup>b</sup>	R <sub>X</sub> <sup>b</sup>	R <sub>R</sub> <sup>c</sup>
EP5	P	91.85	8.15	16.0	–	14.9
EF5	F	50.38	49.62	48.9	55.5	49.7

<sup>a</sup>X = comonomer

<sup>b</sup>Calculated from  $^{29}\text{Si}$  n.m.r. signal intensities of E and X, respectively

<sup>c</sup>Run number calculated for a random distribution

Table 4 Copolymer probability factors and average sequence lengths of poly(DES-co-DPhS) and poly(DES-co-TFPMS)<sup>a</sup>

Polymer	X <sup>b</sup>	P <sub>E-E</sub>	P <sub>E-X</sub>	P <sub>X-E</sub>	P <sub>X-X</sub>	I <sub>E</sub>	I <sub>X</sub>
EP5	P	0.92	0.08	0.96	0.04	11.73	1.04
EP5	F	0.51	0.49	0.49	0.49	2.06	2.03
		(0.45)	(0.55)	(0.56)	(0.44)	(1.82)	(1.79)

<sup>a</sup>Values calculated using  $^{29}\text{Si}$  n.m.r. signal intensities of E (and of X, in parentheses)

<sup>b</sup>X = comonomer

longer-range pentad sequences. Assignment of the triad sequences was based on the assumption that replacement of an ethyl (E) group by trifluoropropylmethyl (F) causes a downfield shift, in analogy to poly(dimethylsiloxane-co-trifluoropropylmethylsiloxane)<sup>5</sup>. Similarly, the upfield region shows the three trifluoropropylmethyl centred triads IV–VI (Table 2).

The copolymer microstructure can be expressed in terms of the run number concept<sup>27</sup>, where the run number (*R*) describes the average number of monomer sequences (runs) in 100 repeating units of a copolymer chain. *R* is related to the  $^{29}\text{Si}$  n.m.r. signal intensities by the following relationship:

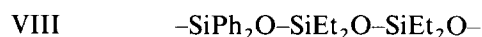
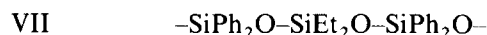
$$R = f_{\text{F}}M_{\text{F}} = f_{\text{E}}M_{\text{E}}$$

where *M<sub>F</sub>* and *M<sub>E</sub>* refer to the mole fractions of the monomeric units E and F in the copolymer, and *f<sub>F</sub>* and *f<sub>E</sub>* are derived from the signal intensity ratios of the F and E triad units in the  $^{29}\text{Si}$  n.m.r. spectrum:

$$f_{\text{E}} = 2[\text{I}/(\text{I} + \text{II} + \text{III})]^{0.5}$$

$$f_{\text{F}} = 2[\text{VI}/(\text{IV} + \text{V} + \text{VI})]^{0.5}$$

The calculated microstructure parameters for the copolymers EF5 and EP5 are shown in Table 3. The experimental *R* values were close to that calculated for a complete random distribution (*R<sub>rand</sub>*), and so therefore the microstructures were assumed to be random. Further microstructure parameters, such as the probability factors, *P<sub>E-E</sub>*, *P<sub>E-X</sub>*, *P<sub>X-E</sub>*, and *P<sub>X-X</sub>* and the average sequence lengths, *I<sub>E</sub>* and *I<sub>X</sub>*, are given in Table 4. The  $^{29}\text{Si}$  n.m.r. spectrum of the copolymer EP5 (Figure 2) consists of two multiplets, corresponding to the diethylsiloxyl and diphenylsiloxyl groups, at  $-(18-22)$  ppm and  $-(45-47)$  ppm, respectively. Considering the downfield region first, and in analogy to the triads I–III, the three diethylsiloxyl-centred triads, VII–IX, are expected:



In fact, three main signals are observed; however, the chemical shift width of this region is too small in comparison to the corresponding triads in poly(dimethylsiloxane-co-diphenylsiloxane)<sup>28</sup>, therefore the signals were assigned in terms of longer-range pentad sequences (Table 5). The signals appearing in the region  $-(20-22)$  ppm are assigned to the type IX pentad structures, IXa–c. Since the copolymer contains a large excess of E units, the pentads IXb and IXc predominate. Pentads corresponding to group VIII are observed at a slightly lower frequency. In this case, the pentad VIIIc is responsible for the major signal at  $-19.5$  ppm, and VIIIb and VIIIc are observed at slightly downfield positions. Due to the small abundance of P units, the pentad VIIIa was not

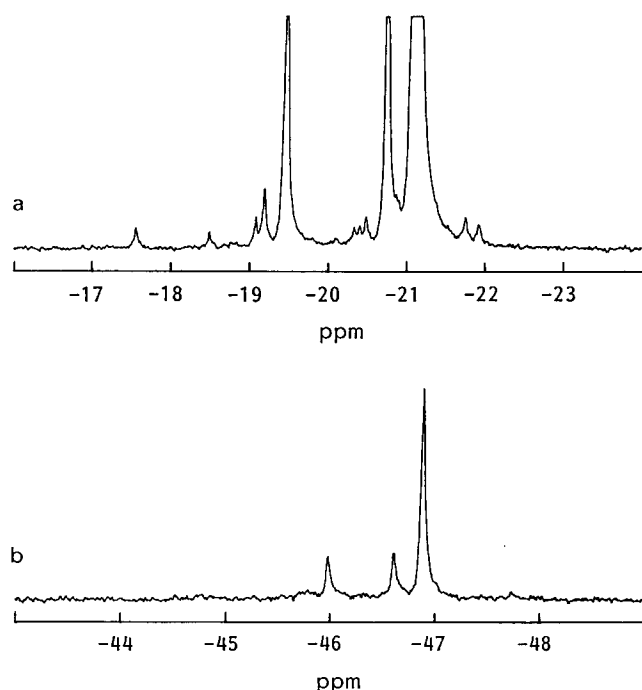


**Figure 2**  $^{29}\text{Si}$  n.m.r. spectrum of the copolymer EP5: (a) diethylsiloxane region; (b) diphenylsiloxane region

**Table 5** Diethylsiloxy-centred pentad sequences in EP copolymers

Pentad	Sequence
VIIa	$-\text{SiPh}_2\text{O}-\text{SiPh}_2\text{O}-\text{SiEt}_2\text{O}-\text{SiPh}_2\text{O}-\text{SiPh}_2\text{O}$
VIIb	$-\text{SiPh}_2\text{O}-\text{SiPh}_2\text{O}-\text{SiEt}_2\text{O}-\text{SiPh}_2\text{O}-\text{SiEt}_2\text{O}$
VIIc	$-\text{SiEt}_2\text{O}-\text{SiPh}_2\text{O}-\text{SiEt}_2\text{O}-\text{SiPh}_2\text{O}-\text{SiEt}_2\text{O}$
VIIIa	$-\text{SiPh}_2\text{O}-\text{SiPh}_2\text{O}-\text{SiEt}_2\text{O}-\text{SiEt}_2\text{O}-\text{SiPh}_2\text{O}$
VIIIb	$-\text{SiEt}_2\text{O}-\text{SiPh}_2\text{O}-\text{SiEt}_2\text{O}-\text{SiEt}_2\text{O}-\text{SiPh}_2\text{O}$
VIIIc	$-\text{SiPh}_2\text{O}-\text{SiPh}_2\text{O}-\text{SiEt}_2\text{O}-\text{SiEt}_2\text{O}-\text{SiEt}_2\text{O}$
VIII d	$-\text{SiEt}_2\text{O}-\text{SiPh}_2\text{O}-\text{SiEt}_2\text{O}-\text{SiEt}_2\text{O}-\text{SiEt}_2\text{O}$
IXa	$-\text{SiPh}_2\text{O}-\text{SiEt}_2\text{O}-\text{SiEt}_2\text{O}-\text{SiEt}_2\text{O}-\text{SiPh}_2\text{O}$
IXb	$-\text{SiPh}_2\text{O}-\text{SiEt}_2\text{O}-\text{SiEt}_2\text{O}-\text{SiEt}_2\text{O}-\text{SiEt}_2\text{O}$
IXc	$-\text{SiEt}_2\text{O}-\text{SiEt}_2\text{O}-\text{SiEt}_2\text{O}-\text{SiEt}_2\text{O}-\text{SiEt}_2\text{O}$

observed, but would be expected for copolymers of higher aromatic content. Not surprisingly, for the type VI triads, only the diethyl-rich pentad VIIc can be clearly discerned from background noise. The signal appearing at  $-17.5$  ppm is thought to arise from the main-chain groups adjacent to the terminal groups.

If the upfield P-centred triad region is considered, it can be seen that such a detailed analysis is not possible due to the poorer S/N ratio, although the E-rich pentads of triads XI and XII can be clearly observed, as follows:

X	$-\text{SiPh}_2\text{O}-\text{SiPh}_2\text{O}-\text{SiPh}_2\text{O}-$
XI	$-\text{SiPh}_2\text{O}-\text{SiPh}_2\text{O}-\text{SiEt}_2\text{O}-$
XII	$-\text{SiEt}_2\text{O}-\text{SiPh}_2\text{O}-\text{SiEt}_2\text{O}-$

Triad X was not observed; therefore, the microstructure parameters for this polymer, given in Tables 3 and 4, could only be calculated from the E-centred triads.

#### D.s.c. studies

The d.s.c. behaviour of high-molecular-weight PDES is complex, with a strong dependence on the thermal history of the sample. In the first study, Lee *et al.* reported

two glass transitions, at  $-60$  and  $-70^\circ\text{C}$ <sup>13</sup>. Adiabatic calorimetry measurements by Beatty and Karasz showed these to be first-order transitions, with a glass transition at approximately  $-143^\circ\text{C}$ <sup>21</sup>. Beatty and Karasz<sup>21</sup> and Godovsky and coworkers<sup>14,15</sup> independently showed that low- and high-temperature double peaks were observed, depending on the cooling rate, and attributed this to crystal dimorphism. Godovsky and coworkers denoted the two dimorphs as  $\alpha_1$  and  $\alpha_2$ , and  $\beta_1$  and  $\beta_2$ , respectively, and suggested that these melt to a phase  $\mu$ , which is birefringent, and thus anisotropic. Since this phase can be sheared like a liquid, it has been described as liquid crystalline or viscous crystalline<sup>17,21,25,29</sup>.

X-ray scattering studies indicated that order was still present above  $27^\circ\text{C}$ <sup>30</sup>. Pochan and coworkers demonstrated via dielectric and proton magnetic relaxation experiments that the onset of motion in the solid occurred at approximately  $-73^\circ\text{C}$ , with translational motion beginning in the range  $-15$  to  $5^\circ\text{C}$ <sup>25,31</sup>. More recently, Moller and coworkers showed that both the  $\alpha$  and  $\beta$  modifications can be distinguished and their transitions monitored by variable temperature  $^{13}\text{C}$  and  $^{29}\text{Si}$  magic angle spinning (MAS) n.m.r. spectroscopy<sup>18</sup>. No motion of the backbone, which would have resulted in a narrowing of the  $^{29}\text{Si}$  chemical shift anisotropy (CSA) was observed below the lower solid–solid transition, although motion involving the side chains was detected. Above this temperature, a considerable upfield change in chemical shift, accompanied by a small change in the  $^{29}\text{Si}$  CSA, led the authors to conclude that conformational disordering occurred with mobility of the  $-\text{SiO}-$  backbone. This was in agreement with Raman studies<sup>22</sup>, and with the d.s.c. studies by Wesson and coworkers<sup>20</sup>, who suggested that the  $\Delta S$  of the transition ( $8.5 \text{ J kmol}^{-1}$ ) was too great to be derived from a crystal–crystal transition.

In our studies, we have prepared a reference sample of PDES (denoted by PDES-1), which shows slightly different crystallization behaviour, depending on the initial cooling rate (Figure 3). When cooled at a rate of  $8^\circ\text{C min}^{-1}$ , two endothermic peaks are observed at  $-73$  and  $-7.5^\circ\text{C}$ , corresponding to the rigid crystal–condensed crystal transition ( $T_d$ ) and the mesophase melting ( $T_m$ ), respectively. In contrast, when the sample is cooled at

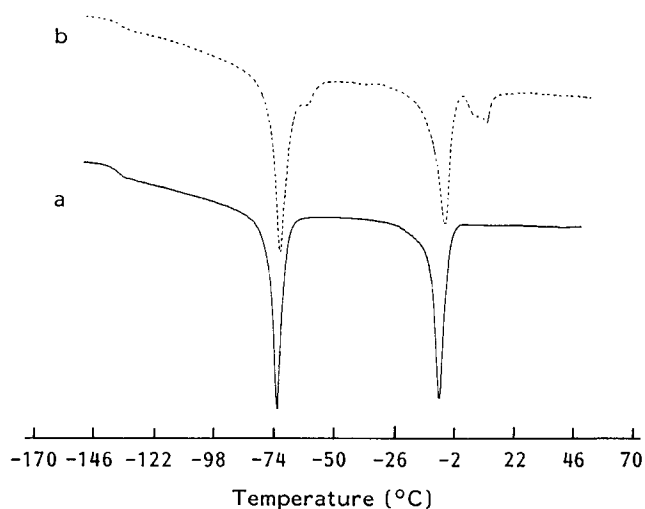


**Figure 3** D.s.c. heating traces of PDES-1: (a) after fast cooling ( $8^\circ\text{C min}^{-1}$ ); (b) after slow cooling ( $2.5^\circ\text{C min}^{-1}$ )

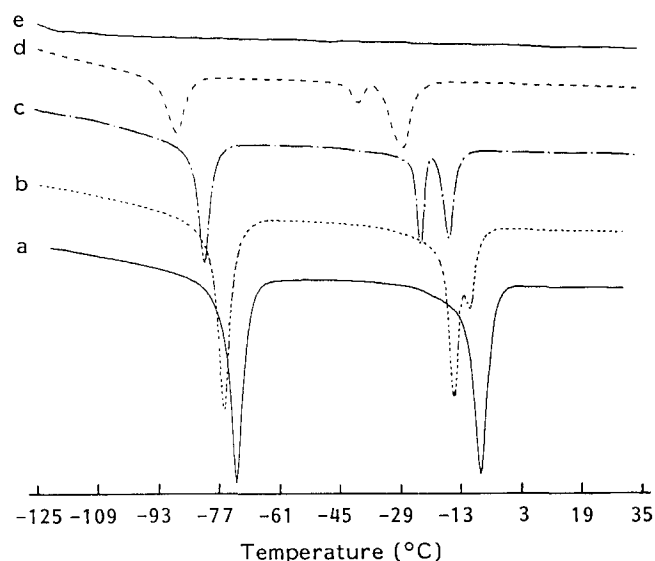


Figure 4 D.s.c. heating of EP copolymers after fast cooling ( $8^{\circ}\text{C min}^{-1}$ ): (a) PDES-1; (b) EP2; (c) EP3; (d) EP4; (e) EP5

$2.5^{\circ}\text{C min}^{-1}$ , additional endotherms at  $-60$ ,  $5.6$  and  $11.6^{\circ}\text{C}$  are observed. These peak temperatures are characteristic of the  $\alpha$  and  $\beta$  phases initially proposed by Godovsky and coworkers<sup>15</sup>. In neither case was any evidence found to indicate the presence of the so termed 'viscous crystalline phase'. This is not unexpected, since the formation of this phase is known to depend strongly on the molecular weight<sup>16</sup>, and those used in this investigation are relatively low.

*D.s.c. of copolymers.* Significant differences were observed in the d.s.c. behaviour of poly(DES-co-DPS) as a function of aromatic content. The d.s.c. traces of polymers EP2, EP3, EP4, EP5 and PDES-1, obtained after a fast cooling rate ( $8^{\circ}\text{C min}^{-1}$ ) are shown in Figure 4. First-order transition temperatures, plus enthalpies and entropies, obtained under conditions of fast ( $8^{\circ}\text{C min}^{-1}$ ) and slow ( $2.5^{\circ}\text{C min}^{-1}$ ) cooling, are listed in Tables 6 and 7, respectively. It can be seen from these results that the effect of increasing the aromatic content

Table 6 D.s.c. crystal transition parameters of poly(DES-co-DPS), obtained under conditions of a fast ( $8^{\circ}\text{C min}^{-1}$ ) cooling rate

Polymer	P content (%)	$T_{\text{onset}}$ ( $^{\circ}\text{C}$ )	$T_{\text{peak}}$ ( $^{\circ}\text{C}$ )	$\Delta H$ ( $\text{J g}^{-1}$ )	$\Delta S$ ( $10^2 \text{ J g}^{-1} \text{ K}^{-1}$ )	Assignment
EP1	0.45	–	8.6	5.1	–	$\alpha_2$ -Isotropic
		–3.5	2.0			$\beta_2$ -Isotropic
		–17.0	–9.6	7.9	3.0	$T_m$
		–74.4	–63.0	17.6	–	$\alpha_1$ – $\alpha_2$
		–78.4	–73.7			$T_d$
EP2	1.00	–16.3	–10.3	10.9	–	$T_{m_2}$
		–17.8	–14.6			$T_{m_1}$
		–79.3	–75.3	10.8	5.4	$T_d$
EP3	2.25	–19.1	–15.5	4.0	1.6	$T_{m_2}$
		–25.4	–23.1	3.3	1.3	$T_{m_1}$
		–83.9	–80.4	9.7	5.0	$T_d$
EP4	4.88	–35.3	–27.7	5.4	2.2	$T_{m_2}$
		–44.1	–39.7	0.8	0.3	$T_{m_1}$
		–94.3	–87.2	5.7	3.1	$T_d$

Table 7 D.s.c. crystal transition parameters of poly (DES-co-DPS), obtained under conditions of a slow ( $2.5^{\circ}\text{C min}^{-1}$ ) cooling rate

Polymer	P content (%)	$T_{\text{onset}}$ ( $^{\circ}\text{C}$ )	$T_{\text{peak}}$ ( $^{\circ}\text{C}$ )	$\Delta H$ ( $\text{J g}^{-1}$ )	$\Delta S$ ( $10^2 \text{ J g}^{-1} \text{ K}^{-1}$ )	Assignment
EP1	0.45	–	8.5	6.6	–	$\alpha_2$ -Isotropic
		–0.1	2.8			$\beta_2$ -Isotropic
		–13.9	–8.6	6.0	2.3	$T_m$
		–74.9	–60.5	15.2	–	$\alpha_1$ – $\alpha_2$
		–74.9	–71.3			$T_d$
EP2	1.00	–14.7	–11.9	9.1	3.5	$T_m$
		–75.6	–73.2	10.7	5.4	$T_d$
EP3	2.25	–	–13.0	7.9	–	$T_{m_2}$
		–19.7	–17.9			$T_{m_1}$
		–77.9	–75.6	9.3	4.7	$T_d$
EP4	4.88	–28.9	–25.7	3.8	1.5	$T_{m_2}$
		–36.7	–34.1	2.6	1.1	$T_{m_1}$
		–86.2	–82.8	5.0	2.6	$T_d$

is to shift both the crystal disordering ( $T_d$ ) and the condensation melting transitions ( $T_m$ ) to lower temperatures, with this being accompanied by a reduction in the heats and entropies of transition. This is clear evidence that the bulky aromatic groups are inhibiting crystallization, and in the case of the copolymer EP5 (P content=8.15%) the polymer is non-crystalline, with a glass transition at  $-127^\circ\text{C}$ .

A second effect of copolymerization is the appearance of the melting peak as a doublet, with the higher-temperature peak (denoted by  $T_{m2}$ ) increasing relative to the lower temperature peak ( $T_{m1}$ ), as a function of the phenyl content. We suggest that this is due to the presence of two similar condensation states, probably differing only by imperfections, although PDES is known to exhibit doublets under such conditions as annealing, etc.<sup>20</sup>.

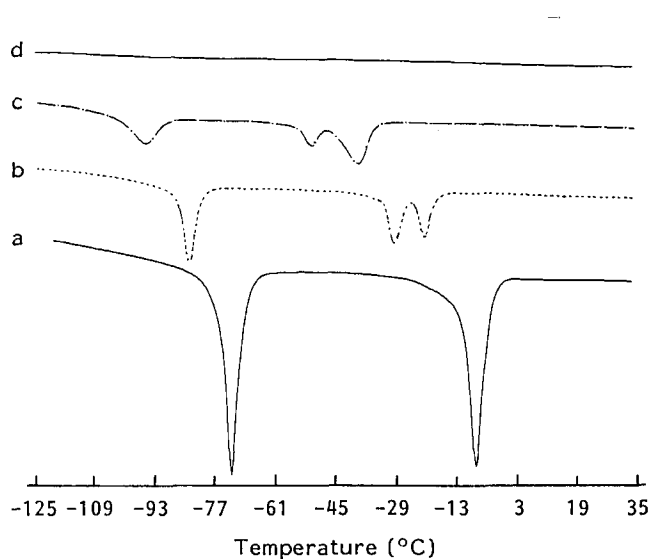


Figure 5 D.s.c. heating traces of EF copolymers after fast cooling ( $8^\circ\text{C min}^{-1}$ ): (a) PDES-1; (b) EF1; (c) EF2; (d) EF4

Analogous results were obtained when the d.s.c. experiments were conducted after slow cooling ( $2.5^\circ\text{C min}^{-1}$ ), although in these cases the peak temperatures are generally higher and the  $T_{m2}$  melting transition is somewhat less dominant. In addition, none of the EP copolymers exhibited a glass transition after slow cooling, thus indicating crystallinities that were close to unity.

The d.s.c. behaviour of poly(DES-co-TFPMS) as a function of F content under conditions of fast cooling (shown in Figure 5) resembles that of the aromatic copolymers. Again,  $T_d$  and  $T_m$  are shifted to a lower temperature, and this is accompanied by the appearance of a second melting peak  $T_{m2}$ . Transition temperatures, plus entropies and enthalpies, are given in Tables 8 and 9, for conditions of fast and slow cooling rates, respectively. The linear relationships of  $T_g$  with composition for poly(DES-co-DPhS) and poly(DES-co-TFPMS), shown in Figures 6 and 7, respectively, further confirm the random nature of the polymer microstructure, since plots with greater curvature would be expected in the case of alternating microstructures.

It is worth noting that polymer EF3 gave rather anomalous d.s.c. behaviour. This copolymer only exhibited a glass transition, and a very small and broad endothermic peak at  $-55^\circ\text{C}$ , with an onset several degrees lower. This signal was reproducible, and in analogy with the other EF copolymers, may be attributed to the condensation-melting transition. This implies that this copolymer is a rare example of a diethylsiloxane-containing polymer which exists in a condensation form, but which cannot crystallize to give a rigid crystal at lower temperatures. The glass transition ( $-133.9^\circ\text{C}$ ) of this copolymer is anomalously low, and does not fit the linear relationship of  $T_g$  and composition which is followed by the remainder of the EF series of copolymers (Figure 7).

Finally, the three amorphous polymers, EF4, EF5 and EP5, gave changes in heat capacity ( $\Delta C_p$ ) of 0.260, 0.247 and  $0.283 \text{ J K}^{-1} \text{ g}^{-1}$ , respectively. If the copolymers are

Table 8 D.s.c. crystal transition parameters of poly(DES-co-TFPMS), obtained under conditions of a fast ( $8^\circ\text{C min}^{-1}$ ) cooling rate

Polymer	F content (%)	$T_{\text{onset}}$ ( $^\circ\text{C}$ )	$T_{\text{peak}}$ ( $^\circ\text{C}$ )	$\Delta H$ ( $\text{J g}^{-1}$ )	$\Delta S$ ( $\text{J g}^{-1} \text{ K}^{-1}$ )	Assignment
EF1	4.21	-24.9	-21.1	8.6	-	$T_{m2}$
		-32.5	-29.1			$T_{m1}$
		-87.0	-83.3	9.2	4.8	$T_d$
EF2	8.40	-47.5	-39.7	6.4	-	$T_{m2}$
		-55.8	-52.2			$T_{m1}$
		-103.4	-95.2	3.2	1.8	$T_d$
EF3	12.20	-62.0	-55.3	0.8	0.4	$T_m$

Table 9 D.s.c. crystal transition parameters of poly (DES-co-TFPMS), obtained under conditions of a slow ( $2.5^\circ\text{C min}^{-1}$ ) cooling rate

Polymer	F content (%)	$T_{\text{onset}}$ ( $^\circ\text{C}$ )	$T_{\text{peak}}$ ( $^\circ\text{C}$ )	$\Delta H$ ( $\text{J g}^{-1}$ )	$\Delta S$ ( $\text{J g}^{-1} \text{ K}^{-1}$ )	Assignment
EF1	4.21	-23.2	-14.0	9.6	-	$T_{m2}$
		-25.8	-21.7			$T_{m1}$
		-85.8	-81.1	8.2	4.3	$T_d$
EF2	8.40	-41.0	-36.2	7.1	-	$T_{m2}$
		-48.9	-44.9			$T_{m1}$
		-100.0	-92.0	4.3	2.4	$T_d$

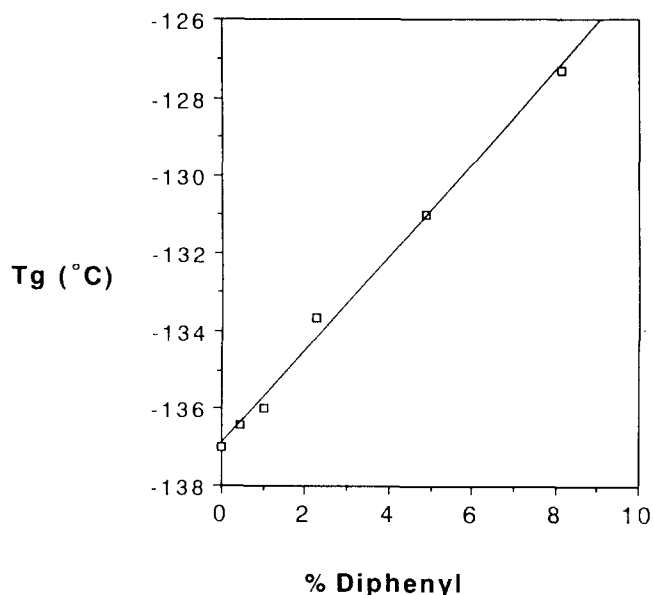


Figure 6  $T_g$ -composition plot for the poly(DES-co-DPhS) series

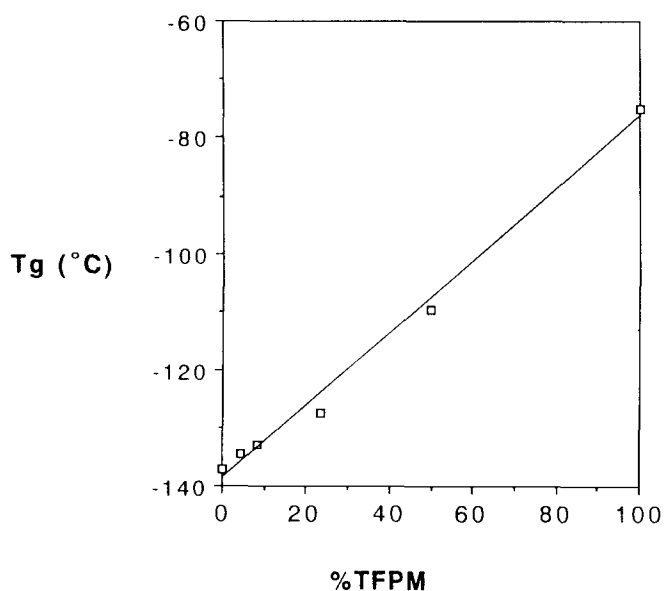


Figure 7  $T_g$ -composition plot for the poly(DES-co-TFPMS) series

considered to have  $E_1F_{0.23}$ , EF and  $E_1P_{0.08}$  repeat units, respectively, the former values correspond, respectively, to molar increases in heat capacity of 35.85, 63.75 and  $33.49 \text{ J K}^{-1} \text{ mol}^{-1}$ . These compare with a predicted value of  $30.65 \text{ J K}^{-1} \text{ mol}^{-1}$  for the PDES homopolymer<sup>20</sup>. Recently, a value of  $34.48 \text{ J K}^{-1} \text{ mol}^{-1}$  has been recommended, following a critical review of the literature<sup>19</sup>.

#### Viscoelasticity

The viscoelastic properties of the copolymers at low temperatures were investigated in order to observe the chain rigidity as a function of temperature. A temperature regime, similar to that employed in the d.s.c. studies, was followed. A plot of the storage modulus and  $\tan \delta$  for PDES-1 as a function of temperature is shown in Figure 8. The most important feature is the lack of a pronounced crystal-condis transition at  $-72^\circ\text{C}$ , which indicates the persistence of considerable order and rigidity in the

condis phase. The condis melting transition  $T_m$  is observed in the form of a double ( $\tan \delta$ ) loss peak in the range  $-1.5$ – $0^\circ\text{C}$ . We believe that the doublet is due to prior complex crystallization under the effect of compression.

In the case of copolymer EF2 (F content of 8.4%), different behaviour is observed (see Figure 9). Due to the extremely high modulus of this sample ( $> 10^{10}$ ) we were unable to take measurements below  $-105^\circ\text{C}$ . Above this temperature a small reorganization peak was observed at  $-93^\circ\text{C}$  (perhaps corresponding to  $T_d$ ). At  $-42^\circ\text{C}$ , a  $\tan \delta$  loss peak, corresponding to  $T_{m1}$ , was observed, followed by another at  $-30^\circ\text{C}$  as a result of the second melting transition. The relative importance of  $T_{m2}$  over  $T_{m1}$ , as demonstrated by the relative losses in the storage modulus  $G'$ , is in agreement with the d.s.c. findings.

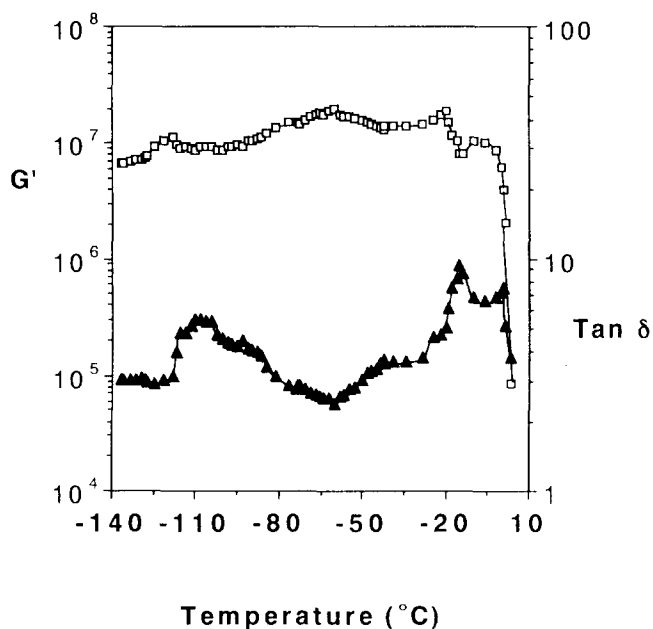


Figure 8 Plot of storage modulus ( $\square$ ) and  $\tan \delta$  ( $\blacktriangle$ ) against temperature for PDES-1

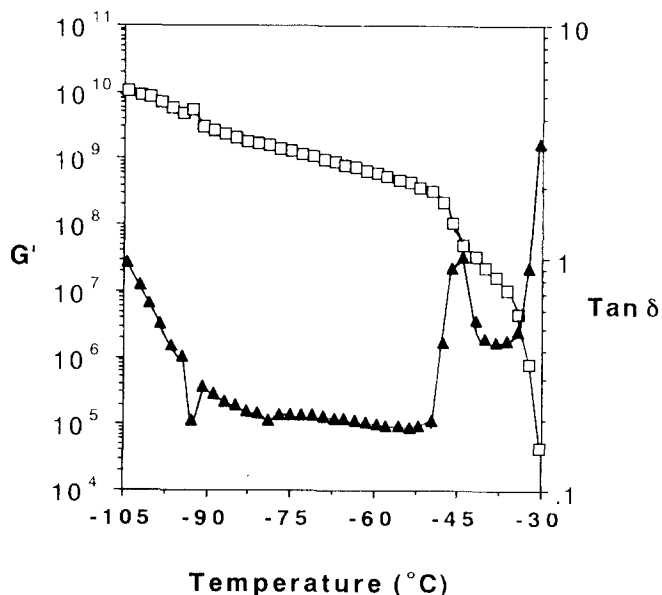


Figure 9 Plot of storage modulus ( $\square$ ) and  $\tan \delta$  ( $\blacktriangle$ ) against temperature for the copolymer EF2

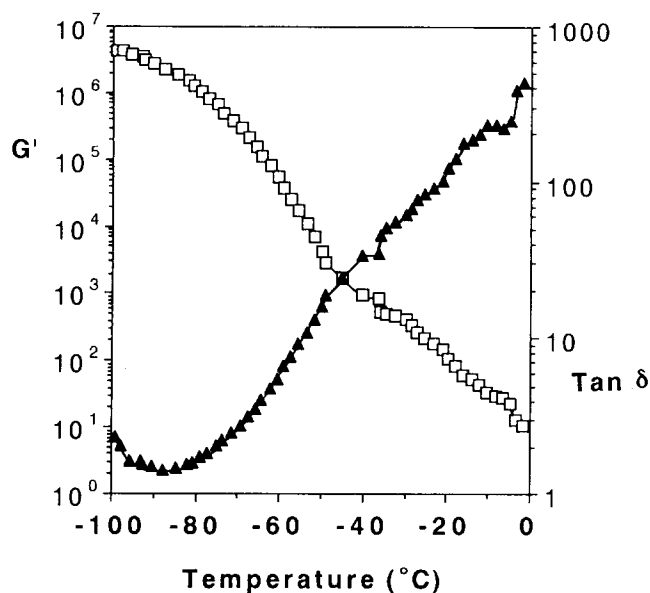


Figure 10 Plot of storage modulus ( $\square$ ) and tan delta ( $\blacktriangle$ ) against temperature for the copolymer EF4

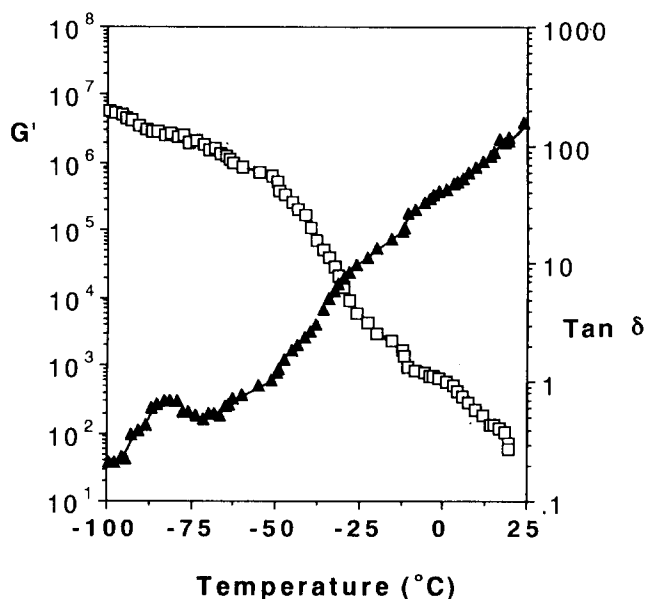


Figure 11 Plot of storage modulus ( $\square$ ) and tan delta ( $\blacktriangle$ ) against temperature for the copolymer EP5

As expected for an amorphous polymer, the non-crystalline copolymer EF4 (F content of 23.4%) shows no major  $\tan \delta$  loss peaks (Figure 10), and  $\tan \delta$  and  $G'$  increase and decrease, respectively, with increasing temperature. A separate experiment showed the presence of a small broad loss peak between  $-115$  and  $-100^\circ\text{C}$ ; however, no signals are observed in the d.s.c. scans at these temperatures, so this is probably an artifact of the  $G''/G'$  ratio.

The copolymers EP4 (4.9% P) and EP5 (8.15% P) show similar behaviour to their EF counterparts. The amorphous polymer EP5 gives a plot (Figure 11) which generally resembles that of copolymer EF5, with no major  $\tan \delta$  loss peaks, while EP4 (Figure 12) exhibits a small  $\tan \delta$  loss peak at  $-83^\circ\text{C}$ , corresponding to  $T_d$ , and further ones at  $-32$  and  $-20^\circ\text{C}$ , due to the condensation melting transitions,  $T_{m1}$  and  $T_{m2}$ , respectively. The fluctuation over the temperature range  $-40$  to  $-50^\circ\text{C}$

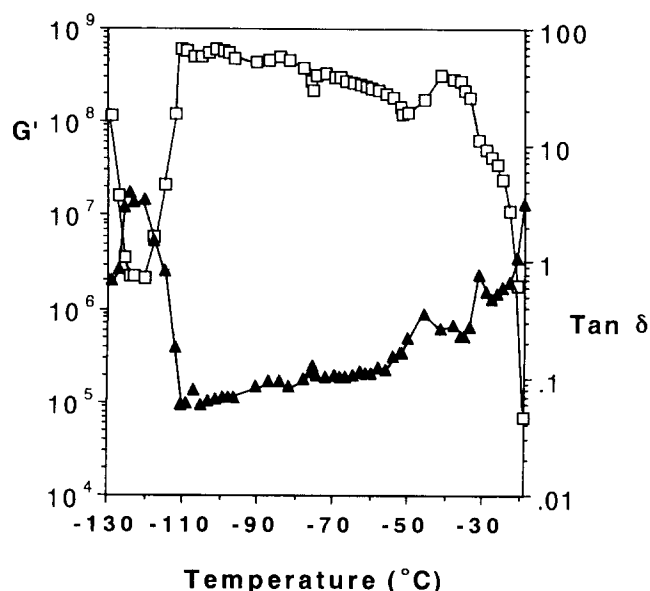


Figure 12 Plot of storage modulus ( $\square$ ) and tan delta ( $\blacktriangle$ ) against temperature for the copolymer EP4

is not understood. In the case of EP4, the  $T_g$  is clearly observed in the range  $-120$  to  $-125^\circ\text{C}$ . This value is some  $5^\circ\text{C}$  higher than that obtained from the d.s.c. experiments, and is expected, since the thermocouple in this technique measures the air temperature around the sample and not the sample itself, thereby giving rise to a small temperature lag.

## CONCLUSIONS

The calorimetric data clearly show the effect of bulky substituents such as phenyl and trifluoropropyl in eliminating crystallinity in these diethylsiloxane polymer systems, presumably by increasing the distance between the ethyl side groups of parallel chains. While as little as 3% diphenyl content has been shown to be effective in inhibiting crystallinity in polydimethylsiloxane<sup>32</sup>, the PDES homologue requires approximately 8%. Moreover, the  $^{29}\text{Si}$  n.m.r. spectroscopy results indicate that an average sequence length of no more than twelve E units is required for the polymer to be amorphous. Increasing the sequence length above this favours crystallization.

The extremely low glass transition temperatures ( $\sim -128^\circ\text{C}$ ) observed for the copolymers EP5 and EF4 are among the lowest published for amorphous polymers and represent an improvement of some  $12$ – $15^\circ\text{C}$  over commercial Silastic elastomers. In view of the relative oxidative instability of the ethyl group at higher temperatures, potential applications of these copolymers probably lie in the low-temperature-elastomer area. Finally, the origin of the two melting transitions,  $T_{m1}$  and  $T_{m2}$ , is not clearly understood, and we are initiating X-ray and solid-state n.m.r. spectroscopic investigations in order to clarify this aspect.

## ACKNOWLEDGEMENTS

The authors are indebted to the Agency of Industrial Science and Technology of Japan for financial support.



## REFERENCES

- 1 Ender, D. H. *CHEMTECH*. 1986, 52
- 2 Hauser, R. L. and Rumpel, W. F. in 'Advances in Cryogenic Engineering' (Ed. K. D. Timmerhaus), Vol. 8, Plenum, New York, 1963, p. 242
- 3 Cornelius, D. J. and Monroe, C. M. *Polym. Eng. Sci.* 1985, **25**, 467
- 4 Saam, J. C. *Adv. Chem. Ser.* 1990, **224**, 71
- 5 Kobayashi, H. and Nishiumi, W. *Makromol. Chem.* 1993, **194**, 1403
- 6 Polmanteer, K. E. and Hunter, M. J. *J. Appl. Polym. Sci.* 1959, **1**, 3
- 7 Godovsky, Y. K., Makarova, N. N., Papkov, V. S. and Kuzim, N. N. *Makromol. Chem. Rapid Commun.* 1985, **6**, 443
- 8 Godovsky, Y. K., Mamaeva, I. I., Makarova, N. N., Papkov, V. S. and Kuzim, N. N. *Makromol. Chem. Rapid Commun.* 1985, **6**, 797
- 9 Moller, M., Siffrin, S., Kogler, G. and Oelfin, D. *Makromol. Chem., Macromol. Symp.* 1990, **34**, 171
- 10 Allcock, H. R. *Angew. Chem.* 1977, **89**, 153
- 11 Sun, D. C. and Magill, J. H. *Polymer* 1987, **28**, 1943
- 12 Schneider, N. S., Desper, C. R. and Beres, J. J. in 'Liquid Crystalline Order in Polymers' (Ed. A. Blumstein), Academic, New York, 1978, p. 299
- 13 Lee, C. L., Johannson, O. K., Flanigan, O. L. and Hahn, P. A. *Chem. Soc. Div. Polym. Chem. Polym. Prepr.* 1969, **10**, 1319
- 14 Papkov, V. S., Godovsky, Y. K., Svistunov, V. S., Litvinov, V. M. and Zhdanov, A. A. *J. Polym. Sci., Polym. Chem. Edn* 1984, **22**, 3617
- 15 Tsvankin, D. Y., Papkov, V. S., Zhukov, V. P., Godovsky, Y. K., Svistunov, V. S. and Zhdanov, A. A. *J. Polym. Sci., Polym. Chem. Edn* 1985, **23**, 1043
- 16 Papkov, V. S., Svistunov, V. S., Godovsky, Y. K. and Zhdanov, A. A. *J. Polym. Sci., Polym. Phys. Edn* 1987, **25**, 1859
- 17 Beatty, C. L., Pochan, J. M., Froix, M. F. and Hinman, D. D. *Macromolecules* 1975, **8**, 547
- 18 Kogler, G., Hasendhndl, A. and Moller, M. *Macromolecules* 1989, **22**, 4190
- 19 Varmar-Nair, M., Wesson, J. P. and Wunderlich, B. *J. Therm. Anal.* 1989, **35**, 1913
- 20 Wiedemann, H. E., Wunderlich, B. and Wesson, J. P. *Mol. Cryst. Liq. Cryst.* 1988, **155**, 469
- 21 Beatty, C. L. and Karasz, F. E. *J. Polym. Sci., Polym. Phys. Edn* 1975, **13**, 971
- 22 Friedrich, J. and Rabolt, J. F. *Macromolecules* 1987, **20**, 1975
- 23 Kogler, G., Loufakis, K. and Moller, M. *Polymer* 1990, **31**, 1538
- 24 Litvinov, V. M., Whittaker, A. K., Hagemeyer, A. and Spies, H. W. *Colloid Polym. Sci.* 1989, **267**, 681
- 25 Pochan, J. M., Beatty, C. L., Hinman, D. D. and Karasz, F. E. *J. Polym. Sci., Polym. Phys. Edn* 1975, **13**, 977
- 26 Miller, K. J., Grebowicz, J., Wesson, J. P. and Wunderlich, B. *Macromolecules* 1990, **23**, 849
- 27 Harwood, H. J. and Ritchey, W. M. *J. Polym. Sci. (B)* 1964, **2**, 601
- 28 Babu, G. N., Christopher, S. S. and Newmark, R. A. *Macromolecules* 1987, **20**, 2654
- 29 Pochan, J. M., Hinman, D. D. and Froix, M. F. *Macromolecules* 1976, **9**, 611
- 30 Papkov, V. S., Godovsky, Y. K., Svistunov, V. S., Litvinov, V. M. and Zhdanov, A. A. *J. Polym. Sci., Polym. Phys. Edn* 1984, **22**, 3617
- 31 Froix, M. F., Beatty, C. L., Pochan, J. M. and Hinman, D. D. *J. Polym. Sci., Polym. Phys. Edn* 1975, **13**, 1269
- 32 O'Malley, W. J. *Adhes. Age* 1975, **18**(6) 17